

Line-shape analyses of magnon Raman spectra of a $\text{PrBa}_2\text{Cu}_{2.7}\text{Al}_{0.3}\text{O}_7$ single crystal

M. Rübhausen, N. Dieckmann, A. Bock, and U. Merkt

*Institut für Angewandte Physik und Zentrum für Mikrostrukturforschung,
Universität Hamburg, Jungiusstrasse 11, 20355 Hamburg, Germany*

(Received 17 June 1996)

We present line-shape analyses of magnon Raman spectra in B_{1g} geometry of a $\text{PrBa}_2\text{Cu}_{2.7}\text{Al}_{0.3}\text{O}_7$ crystal for various excitation energies. The description is based on the Heisenberg model of antiferromagnetism. Out of resonance, we describe the experimental data by taking into account phonons and a two-magnon excitation using the experimental superexchange energy $J=720\text{ cm}^{-1}$ and a damping parameter $\Gamma=200\text{ cm}^{-1}$ of the one-magnon states. After subtraction of the fitted line shapes, we identify three additional spectral features at 730 cm^{-1} , 1170 cm^{-1} , and 3500 cm^{-1} . All three show enhanced intensities close to the two-magnon resonance at 2.79 eV excitation energy. This strongly suggests that these excitations have a magnetic rather than a phononic origin. [S0163-1829(96)05945-0]

In the last few years significant progress in the interpretation of magnon Raman spectra of high-temperature superconductor parent phase antiferromagnets has been achieved. In particular, resonant theories¹⁻³ have provided new ideas of the complex processes taking part in the interaction of light with the copper-oxygen planes of, e.g., $\text{YBa}_2\text{Cu}_3\text{O}_6$, LaCuO_4 , and $\text{PrBa}_2\text{Cu}_3\text{O}_7$. Qualitatively, resonant theories³ based on a one-band Hubbard model have been confirmed for $\text{PrBa}_2\text{Cu}_3\text{O}_7$,⁴ $\text{YBa}_2\text{Cu}_3\text{O}_6$, and SrCuOCl .⁵ As far as the line shape is concerned, Shastry and Shraiman¹ have shown that out of resonance and in B_{1g} geometry the scattering Hamiltonian can be described by the classical Hamiltonian of Fleury and Loudon⁶ based on the Heisenberg model of antiferromagnetism (HAFM). However, in resonance additional contributions have to be considered. In this Brief Report we analyze line shapes of Raman spectra of a $\text{PrBa}_2\text{Cu}_{2.7}\text{Al}_{0.3}\text{O}_7$ single crystal based on the HAFM. In resonance, the observed line shapes reveal three additional features, which cannot be described in the conventional framework.^{7,8} We have published the calibration-corrected data in a previous paper to which we refer for experimental details.⁴

We follow the approach of Canali and Girvin.⁷ Starting with the HAFM and carrying out the standard Dyson-Maleev and Bogoliubov transformations, they find within the random phase approximation (RPA) the intensity

$$I(\omega) = \text{Im}[G(\omega)], \quad (1)$$

with the response function

$$G(\omega) = \frac{G^0(\omega)}{1 + (1/Sz\alpha J)G^0(\omega)}. \quad (2)$$

Here J is the superexchange energy, $z=4$ the number of nearest neighbors, $S=\frac{1}{2}$ the spin value, and α is the Oguchi factor,⁹ which equals 1.16 for two-dimensional systems.⁷ The function

$$G^0(\omega) = \sum_k \frac{f_k^2 \epsilon_k}{(\omega - 2\epsilon_k + 2i\Gamma)(\omega + 2\epsilon_k + 2i\Gamma)} \quad (3)$$

is determined by the dispersion relation

$$\epsilon_k = \sqrt{1 - \frac{1}{4}[\cos(k_x a) + \cos(k_y a)]^2}, \quad (4)$$

the factor $f_k = \frac{1}{2}[\cos(k_x a) - \cos(k_y a)]$ representing the B_{1g} geometry and a phenomenological damping parameter Γ similar to the one introduced by Weber and Ford.⁸ Equations (1)–(4) can be evaluated by direct numerical integration¹⁰ across the antiferromagnetic Brillouin zone.

Experimental data taken in B_{1g} geometry with 2.41 eV excitation energy at 14 K and theoretical line shapes are shown in Fig. 1(a). The spectrum consists of three different contributions. First, we have the magnon line, which participates in the low-energy range and dominates the high-energy range with a peak near 2310 cm^{-1} . The observed decrease of the scattering intensity for large Raman shifts simplifies the theoretical description. Sometimes, residual scattering signal for large Raman shifts is reported. However, its origin is unclear and its observed line shape varies significantly for the same compound, e.g., $\text{YBa}_2\text{Cu}_3\text{O}_{6+x}$.^{5,11-13} Second, we find phonon peaks up to 650 cm^{-1} due to first-order phonon scattering.^{14,15} Finally, there is a stray-light background, which has a significant contribution only below 800 cm^{-1} . The luminescence observed in Ref. 4 has been subtracted here. The fitted line shapes have been obtained by the following procedure. We have computed the two-magnon line shape disregarding phonons and stray light. Next the two-magnon scattering intensity has been subtracted from the experimental data. Then, we have fitted the phonons using a stray-light background. Residual scattering intensity of the magnons can be found in the phononic regime. In Fig. 1(b) we plot the low-energy range of the spectrum up to 1400 cm^{-1} . In total we find eight phonons contributing to this part of the spectrum. Two of them allow a straightforward interpretation. The dominating phonon in B_{1g} geometry is the O(2)-O(3) vibration of the plane oxygen at 302 cm^{-1} . The phonon at 509 cm^{-1} of the O(4) vibration is weak in this scattering geometry. Due to the substitution of aluminum¹⁶ for copper, the inversion symmetry is partly broken and three infrared-active and disorder-induced modes appear at 175 cm^{-1} , 220 cm^{-1} , and 580 cm^{-1} . Similar modes have been observed in $\text{YBa}_2\text{Cu}_3\text{O}_{6.5}$.¹⁷ Finally, the three remaining

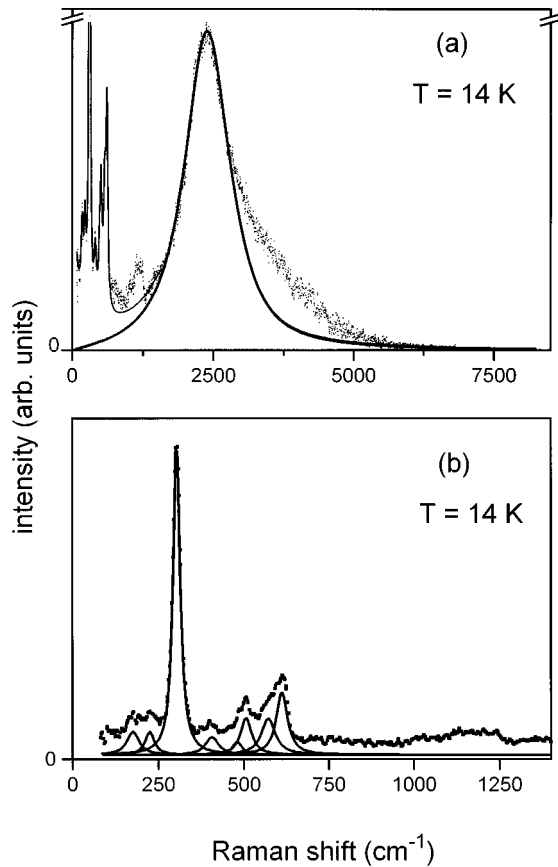


FIG. 1. (a) Raman spectrum in B_{1g} geometry (dots) taken with an excitation energy of 2.41 eV at 14 K and fits to the data (solid lines) using the HAFM model, phonons, and a stray-light background. The phonon at 302 cm^{-1} is not displayed in full strength. (b) Low-energy regime displaying the phonons in detail.

phonons at 406 cm^{-1} , 480 cm^{-1} , and 612 cm^{-1} have no relation to the aluminum substitution, as we find them in aluminum-free samples as well. Their origin is presently unknown, but we would like to point out that several authors have found crystal-field excitations of Pr^{+3} in the low-energy region.^{18–20} On the other hand, as they have a similar width and strength as weak phonon excitations a detailed temperature- and symmetry-dependent investigation has to be carried out in order to identify the origin of these peaks.

In Fig. 2(a) we show experimental data for an excitation energy of 2.54 eV and the corresponding fits at 300 K, which is above the Néel temperature $T_N \approx 280\text{ K}$.²¹ The fit describes the data quite well. This is shown in Fig. 2(b), where the upper and lower curves correspond to a subtraction of the fit from the experimental data at 14 K and 300 K, respectively. Whereas structures between 730 cm^{-1} and 1200 cm^{-1} are visible at both temperatures, the high-energy tail is significantly reduced at the higher one. As can be seen in Table I, we find the same exchange energy but an increased damping parameter at 300 K. From the damping parameter we are able to make a rough estimate of the size in which an antiferromagnetic correlation exists.⁸ For the 14 K and the 300 K measurements we estimate 2.3 nm and 0.9 nm, respectively. At 14 K this corresponds to an array of about 13×13 spins. In contrast to this, the 300 K value corresponds to an array of

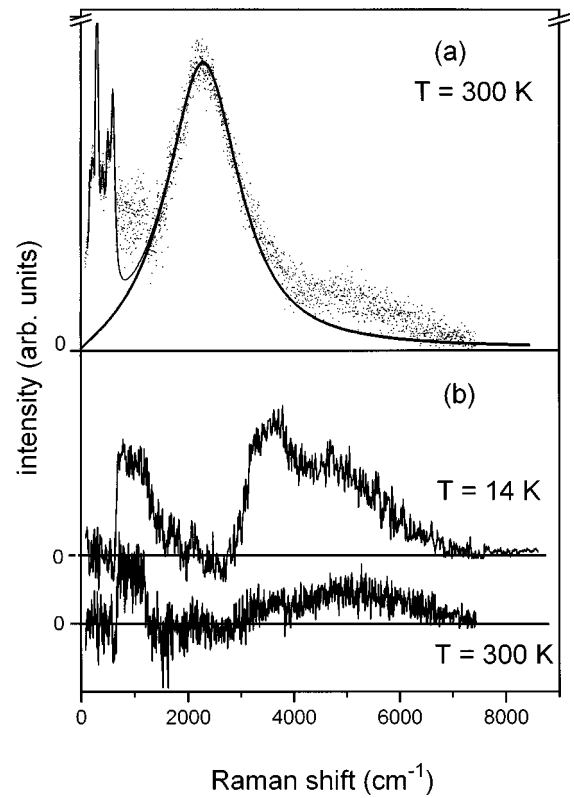


FIG. 2. (a) Raman spectra in B_{1g} geometry (dots) taken with an excitation energy of 2.54 eV at 300 K and fits to the data (solid lines). The phonon at 302 cm^{-1} is not displayed in full strength. (b) Residual signals after subtraction of the fit from the experimental data at 300 K and 14 K.

only 4×4 spins. The latter might be too small for four-magnon excitations, which we assume to be responsible for the high-energy tail. Four-magnon excitations occur at energies of $4J$, $5J$, $6J$, $7J$, and $8J$ in a simple spin-flip picture. The required size of the antiferromagnetic cluster increases with increasing energy.⁴ The $8J$ process involves at least an array of 6×6 spins, whereas the $4J$ process can occur already on a 4×4 array. Therefore completely vanished intensities of four-magnon excitations with higher energies can be expected, whereas the four-magnon $4J$ process is supposed to be strongly damped.

At first sight it might seem that the strength of the two-magnon peak in the paramagnetic regime and its proper de-

TABLE I. Damping parameter Γ and exchange energy J of the two-magnon line for various excitation energies and two temperatures.

Excitation energy (eV)	T (K)	J (cm^{-1})	Γ (cm^{-1})
2.41	14	711	188
2.46	14	720	217
2.54	14	718	200
2.60	14	713	215
2.70	14	733	310
2.54	300	720	350

scription is quite surprising. We apply a $T=0$ theory for an antiferromagnetic system in the paramagnetic regime, where the usual requirements of the theoretical descriptions cannot be expected to hold. For traditional two-dimensional HAFM systems, like K_2NiF_4 , it is well known that the two-magnon peak still persists for temperatures up to $T=3T_N$ and the quasiparticle approach might be applied for temperatures of the order of T_N .²² This is a consequence of the strong momentum dependence of the quasiparticle renormalization in the HAFM. Excitations originating from the antiferromagnetic Brillouin zone boundary require only short-range order; thus changes of the long-range order have weak effects on the two-magnon excitations. It is worthwhile to remark that the experimentally observed renormalization in three-dimensional systems is different from the two-dimensional case. In three dimensions like in KNiF_3 , the linewidth is increased by a factor of 2.5 and the peak position is shifted to smaller frequencies by a factor of 0.2 at $T=T_N$ compared to $T=0$.²² In two-dimensional systems like in K_2NiF_4 , one can find an increase of the linewidth by a factor 1.7, whereas the peak position is only shifted to smaller frequencies by a factor of 0.95.²² At $T=T_N$, we find a damping parameter increased by a factor of 1.75 ± 0.05 together with a renormalization of the peak position by a factor of 0.97 ± 0.03 . Therefore, $\text{PrBa}_2\text{Cu}_{2.7}\text{Al}_{0.3}\text{O}_7$ shows an ideal two-dimensional behavior as we observe quantitatively the same renormalization as for K_2NiF_4 . From the line-shape analyses of the 14 K spectra,⁴ we obtain values of $J=720 \text{ cm}^{-1}$ and $\Gamma=200 \text{ cm}^{-1}$ independent of the excitation energy up to 2.60 eV as shown in Table I. However, at 2.70 eV and 14 K the HAFM cannot be applied as can be seen by the unphysically large damping parameter and exchange energy. The spectra obtained by subtracting the fit from the experimental data are shown in Fig. 3. Three different signals appear in resonance. The first two structures are centered around 730 cm^{-1} and 1170 cm^{-1} . The third feature has its maximum at 3500 cm^{-1} . The inset shows the spectra for 2.60 eV and 2.70 eV laser excitation energy, when a two-magnon peak of $J=720 \text{ cm}^{-1}$ and $\Gamma=200 \text{ cm}^{-1}$ is subtracted. The inset reveals the breakdown of the HAFM model when the excitation energy almost matches the resonance position, which we have found to be 2.79 eV in this system.⁴ The spectral weight of the residual signal becomes much larger compared to the lower excitation energies. In particular, there should be no dependence of the one-magnon damping parameter Γ on the excitation energy. A straightforward fit only poorly describes the line shape and yields a damping parameter increased by a factor of 1.5. To investigate the resonance behavior of the three features we plot their inverse peak heights versus the laser excitation energy in Figs. 4(a) and 4(b). In Fig. 4(a) we show the two-magnon resonance as well as the resonance behavior of the peak at 3500 cm^{-1} . The resonance position $\hbar\omega_1=2.73 \text{ eV}$ of the peak seems to be slightly lower than the two-magnon process at $\hbar\omega_2=2.79 \text{ eV}$. However, the uncertainty of the $\hbar\omega_1$ value is much larger than the one for the two-magnon resonance energy $\hbar\omega_2$. Within the experimental error both peaks become resonant at basically the same energy. From this we conclude that the peak at 3500 cm^{-1} is likely to be related to four-magnon excitations. This interpretation is also supported by the observation of its strong temperature dependence and the slope of the inverse peak

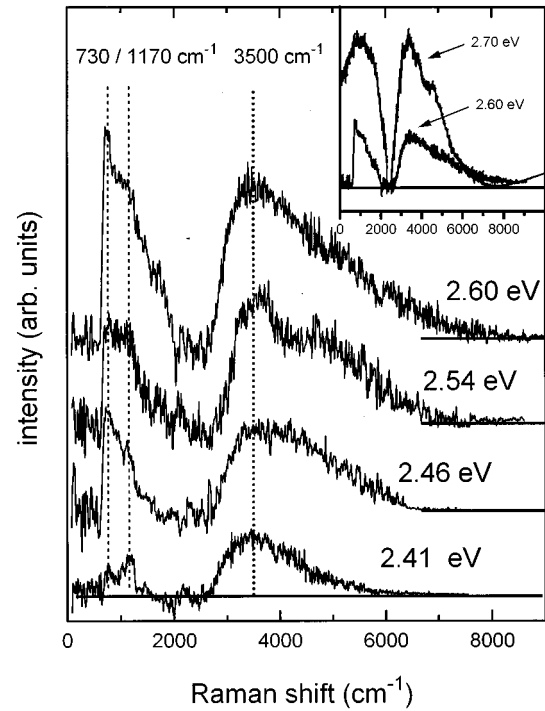


FIG. 3. Residual signals for various excitation energies. The inset shows the residual signals at 2.60 and 2.70 eV, demonstrating the breakdown of the HAFM model. Peak positions of the spectral features at 730 cm^{-1} , 1170 cm^{-1} , and 3500 cm^{-1} are indicated.

heights. The slope is observed to be larger by a factor of 5–6 in the four-magnon case. Chubukov and Frenkel^{2,3} have pointed out that in resonance one additional contribution might result from noninteracting magnons with an energy of $4J$. However, an assignment of the peak at 3500 cm^{-1} to this $4J$ excitation is unlikely, because of the peak position of $4.9 J$ and the extent of the spectral feature that reaches energies of $8 J$.⁴

The features at 730 cm^{-1} and 1170 cm^{-1} also show a nearly linear behavior of their reciprocal intensity as shown

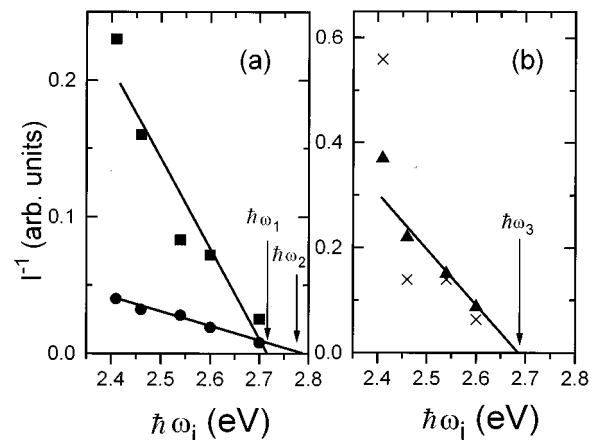


FIG. 4. Inverse peak heights of the two-magnon (circles) and of the residual spectral features at 3500 cm^{-1} (squares), 1170 cm^{-1} (triangles), and 730 cm^{-1} (crosses). Solid lines are linear fits.

in Fig. 4(b). However, the fit for the 1170 cm^{-1} feature yields a value of the resonance energy of 2.68 eV . From the temperature dependence we are not able to assign this signal to a spin-wave origin directly. On the other hand, when we take into account the weak renormalization of the two-magnon peak we cannot exclude such an origin. A phononic origin is unlikely, because of their resonance and symmetry properties.²³ An identification of these peaks might be found in a more detailed analysis of the possible two-magnon diagrams, as a complete evaluation of all diagrams in resonance is still missing.

To summarize, we have carried out line shape analyses of magnon Raman spectra of a $\text{PrBa}_2\text{Cu}_{2.7}\text{Al}_{0.3}\text{O}_7$ single crystal in B_{1g} geometry at 14 K and 300 K . Out of resonance we find good agreement with the predictions of the HAFM model. This leads at 14 K to values of $J=720\text{ cm}^{-1}$ and $\Gamma=200\text{ cm}^{-1}$. At 300 K above the Néel temperature of $T_N\approx 280\text{ K}$ when the high-energy tail has vanished, we find a better description of the line shape with values $J=720\text{ cm}^{-1}$ and $\Gamma=350\text{ cm}^{-1}$. This renormalization at 300 K supports a strictly two-dimensional model. Subtracting the fitted spectra, we find three additional signals at 730

cm^{-1} , 1170 cm^{-1} , and 3500 cm^{-1} , which increase close to resonance and indicate a breakdown of the HAFM model. The inverse peak heights of the 1170 cm^{-1} and 3500 cm^{-1} features follow a straight line leading to resonance positions of 2.68 eV and 2.73 eV , respectively. The 3500 cm^{-1} peak can be assigned to four-magnon processes. This is supported by the peak position, its negligible intensity above the Néel temperature, and its resonance behavior. The origin of the two signals at 730 cm^{-1} and 1170 cm^{-1} remains unknown, but might be found in a diagrammatic approach of Raman scattering in one-band Hubbard systems.

We would like to thank W. Widder and E. Holzinger-Schweiger for providing us with samples as well as D. Manske and C. T. Rieck for encouraging discussions on the theory of Raman scattering in Hubbard systems. We acknowledge financial support from the Bundesministerium für Forschung, Bildung, Technologie und Zukunft, Germany, under Contract No. 13N5807A. M.R. acknowledges a grant from the Graduiertenkolleg Physik nanostrukturierter Festkörper of the Deutsche Forschungsgemeinschaft.

-
- ¹B.S. Shastry and B.I. Shraiman, *Int. J. Mod. Phys. B* **5**, 365 (1991).
- ²A.V. Chubukov and D.M. Frenkel, *Phys. Rev. Lett.* **74**, 3057 (1995).
- ³A.V. Chubukov and D.M. Frenkel, *Phys. Rev. B* **52**, 9760 (1995).
- ⁴M. Rübhausen, N. Dieckmann, A. Bock, U. Merkt, W. Widder, and H.F. Braun, *Phys. Rev. B* **53**, 8619 (1996).
- ⁵G. Blumberg, P. Abbamonte, M.V. Klein, W.C. Lee, D.M. Ginsberg, L.L. Miller, and A. Zibold, *Phys. Rev. B* **53**, R11 930 (1996).
- ⁶P.A. Fleury and R. Loudon, *Phys. Rev.* **166**, 514 (1968).
- ⁷C.M. Canali and S.M. Girvin, *Phys. Rev. B* **45**, 7127 (1992).
- ⁸W.H. Weber and G.W. Ford, *Phys. Rev. B* **40**, 6890 (1989).
- ⁹T. Oguchi, *Phys. Rev.* **117**, 1151 (1960).
- ¹⁰P.J. Davis and P. Rabinowitz, in *Methods of Numerical Integration*, Computer Science and Applied Mathematics, edited by W. Rheinboldt (Academic, New York, 1975).
- ¹¹S. Sugai, M. Sato, T. Ito, T. Ido, H. Takagi, S. Uchida, T. Kobayashi, J. Akimitsu, Y. Hidaka, T. Murakami, S. Hosoya, T. Kajitani, and T. Fukuda, *Physica B* **165-166**, 1263 (1990).
- ¹²G. Blumberg, R. Liu, M.V. Klein, W.C. Lee, D.M. Ginsberg, C. Gu, B.W. Veal, and B. Dabrowski, *Phys. Rev. B* **49**, 13 295 (1994).
- ¹³M. Mayer, P. Knoll, M. Pressl, S. Lo, and E. Holzinger-Schweiger, *Physica C* **235-240**, 1097 (1994).
- ¹⁴H.B. Radousky, K.F. McCarty, J.L. Peng, and R.N. Shelton, *Phys. Rev. B* **39**, 12 383 (1989).
- ¹⁵J. Humlíček, A.P. Litvinchuk, W. Kress, B. Lederle, C. Thomsen, M. Cardona, H.-U. Habermeier, I.E. Trofimov, and W. König, *Physica C* **206**, 345 (1993).
- ¹⁶W. Widder, M. Stebani, L. Bauernfeind, H.F. Braun, K. Widder, H.P. Gesserich, M. Rübhausen, N. Dieckmann, and A. Bock, *Physica C* **256**, 168 (1996).
- ¹⁷M. Iliev, C. Thomsen, V. Hadjiev, and M. Cardona, *Phys. Rev. B* **47**, 12 341 (1993).
- ¹⁸M.L. Sanjuán and M.A. Laguna, *Phys. Rev. B* **52**, 13 000 (1995).
- ¹⁹J.A. Sanjurjo, C. Rettori, S. Oseroff, and Z. Fisk, *Phys. Rev. B* **49**, 4391 (1994).
- ²⁰K. Nehrke and M.W. Pieper, *Phys. Rev. Lett.* **76**, 1936 (1996).
- ²¹D.W. Cooke, R.S. Kwok, R.L. Lichti, M.S. Jahan, T.R. Adams, C. Boekema, W.K. Dawson, A. Kebede, J. Schwegler, J.E. Crow, and T. Mihalisin, *Physica B* **163**, 675 (1990).
- ²²U. Balucani and V. Tognetti, *Rev. Nuovo Cimento* **6**, 39 (1976).
- ²³M. Mayer, P. Knoll, and E. Holzinger-Schweiger, *J. Supercond.* (to be published).